



Interaction fluide structure appliquée a l'analyse des voiles

Daniele Trimarchi, Stephen Turnock, Dominic Taunton, Dominique Chapelle,
Marina Vidrascu

► To cite this version:

Daniele Trimarchi, Stephen Turnock, Dominic Taunton, Dominique Chapelle, Marina Vidrascu. Interaction fluide structure appliquée a l'analyse des voiles. 10e colloque national en calcul des structures, May 2011, Giens, France. 8 p. hal-00592960

HAL Id: hal-00592960

<https://hal.archives-ouvertes.fr/hal-00592960>

Submitted on 3 May 2011

HAL is a multi-disciplinary open access archive for the deposit and dissemination of scientific research documents, whether they are published or not. The documents may come from teaching and research institutions in France or abroad, or from public or private research centers.

L'archive ouverte pluridisciplinaire **HAL**, est destinée au dépôt et à la diffusion de documents scientifiques de niveau recherche, publiés ou non, émanant des établissements d'enseignement et de recherche français ou étrangers, des laboratoires publics ou privés.

Fluid Structure Interactions applied to Downwind Yacht Sails

D. Trimarchi¹, M. Vidrascu², D. Taunton¹, S.R. Turnock¹,
D. Chapelle²

¹ Fluid Structure Interactions Research Group, University of Southampton, United Kingdom, daniele.trimarchi@soton.ac.uk

² INRIA, MACS team, France

Abstract — Sail analysis is a rapidly evolving field, since it has a big impact in the performances of yachts. In the present approach, a weak coupling in Arbitrary Lagrangian Eulerian (ALE) configuration has been chosen. The flow is analyzed with a Reynolds Averaged Navier Stokes (RANS) Finite Volume (FV) solver with turbulence models, whereas the structural analysis is performed with non-linear MITC Shell Finite Elements (FE). The approach and examples are presented and discussed with regards to a two dimensional downwind sail section in turbulent flow.

Keywords — Sail analysis, RANSE, Finite Elements, Fluid Structure Interactions.

1 Introduction

Downwind sail analysis is particularly complex because of the number of phenomena interacting together. From a fluid perspective, sails are thin laminates operating in a wide range of angles of attack. Because of the large angle of attack and the device curvature the force generation results in an intermediate regime of lift and drag, with large regions of separated flow. Due to the size and the relevant wind speed, transition to turbulent flow arises in the very first part of the device, behind the leading edge. Due to adverse pressure gradients and the sharp corner leading edge, separation bubbles are likely to form on the edges of the device, thus further increasing the flow complexity.

Unsteady phenomena can be driven by a composition of fluid unsteadiness such as the vortex shedding, and unsteadiness induced by the boat's motions in seaway or the gusts. The impact of unsteady flows can be identified in a global increase in the force generation process [12].

In the approach presented here the flow is simulated with a Finite Volume (FV) approach. The C++ library OpenFOAM [7] has been chosen, since it includes unsteady RANS solvers and the most commonly adopted turbulence models, as well as dynamic mesh handling capabilities.

From a structural point of view sails are constituted by thin orthotropic laminates, which can be assumed to be in large displacements-small strains regime. Since sails are made of fabrics, wrinkling may appear. This is a buckling related phenomenon, which determines the formation of oscillations and wrinkles onto the fabric surface. Since Wrinkling locally modify stress distributions in the fabric, it may have strong influence on the whole deformed equilibrium shape.

Due to its computational cost, only a few authors approached coupled fluid structure interaction (FSI) analysis of downwind sails. In such works, the flow is generally modelled with FV Methods for the solution of RANS equations [8], and SST turbulence model [3]. Downwind sail fluid structure interactions have been presented, where a weak steady coupling is performed between RANS and FE solvers [9]. From a structural perspective, the sailcloth is usually analyzed with CST membranes [4]. Such elements derive from a rather simplified formulation, based on the geometrical observation that a triangle is uniquely defined by the sides length, therefore that the element's strain can be entirely evaluated using such measure.

Furthermore, due to the lack of bending stiffness, the membrane model is inadequate to deal with some particular situations, in particular when wrinkling occurs. Wrinkling being buckling related, its development is in fact completely controlled by the bending stiffness. The membrane model results in such cases undetermined, and strong singularities may appear and affect the solution. The problem is generally overcome with ad-hoc wrinkling models, the scope of which is to modify the constitutive

relationship when a wrinkling criterion is satisfied.

In the present approach the sail fabric is simulated with the use of non-linear shells of the Mixed Interpolation Tensorial Components (MITC) family [2]. Compared to membranes, the shell model includes the bending stiffness, thus all the relevant strain components are represented. This assures that the model is never undetermined, thus wrinkling is directly represented without the need of additional models [14, 13]. The MITC shells has been chosen, since this particular model is formulated for avoiding numerical locking, a phenomenon arising and affecting results in the analysis of thin shells. The structural analysis is carried out with Shelddon, a Fortran Finite Element (FE) package developed by INRIA and allowing the use of non-linear shells MITC.

Fluid structure coupling is performed in an Arbitrary Lagrangian Eulerian (ALE) framework using the dynamic mesh capabilities of OpenFOAM. Data are passed between fluid and structure framework using openMPI, already adopted in OpenFOAM for high performance parallel computing purposes.

2 Methods

The fluid analysis is carried out with the FV C++ library OpenFOAM. Two main solvers have been used for fluid analysis and FSI. In the first case, the pisoFOAM solver has been chosen. This is a semi-implicit uncoupled solver for transient incompressible flows. It is based upon the FV discretization of the Navier-Stokes equations. FSI coupled analysis has been carried out using the PimpleDyMFOAM solver. This solver allows the use of dynamic meshes in ALE framework, thus it makes possible conservative movements of mesh regions within the fluid domain. The standard solver has been modified by the author in order to impose the boundary movement specified by the structural solver, and allow the data communication via MPI. In both cases the SST turbulence model has been chosen. This is a blend of κ - ϵ and κ - ω models [6], which is generally considered one of the best compromises for sail type flows [3].

The structural analysis is performed with the Shelddon finite element library [11]. The sail fabric is represented by non-linear four nodes MITC shells. An isotropic linear elastic constitutive relationship has been chosen, since a small strain regime is assumed. The use of shells rather than membranes has the advantage that no additional models are required for the treatment of wrinkling, which can be represented directly [12]. Severe convergence issues may arise, due to the very limited thickness of the fabric, which cause the system to be very ill conditioned. This problem has been overcome using a dynamic routine with Rayleigh Damping, the details of which can be found in [12]. For completeness however, the basic equations are reported below. By discretization with the mid-point rule, the structural dynamic governing equation reads, in a linear framework:

$$\left(\frac{4\mathbf{M}}{\delta t^2} + \frac{2\mathbf{C}}{\delta t} + \mathbf{K}_T \right) \cdot y_{n+\frac{1}{2}} = \left(\frac{4\mathbf{M}}{\delta t^2} + \frac{2\mathbf{C}}{\delta t} \right) \cdot y_n + \frac{2\mathbf{M}}{\delta t} \cdot \dot{y}_n + F_{n+\frac{1}{2}} \quad (1)$$

where:

\mathbf{M} , \mathbf{C} , \mathbf{K}_T are the structure's mass, damping and tangent stiffness matrices

δt is the time-step

y_n, \dot{y}_n are the position and velocity vectors at the time-step n $\dot{y}_{n+\frac{1}{2}} = \frac{(y_{n+1} + y_n)}{2}$

Mass and Stiffness matrices definition can be found in [1], whereas Rayleigh definition of damping has been chosen. The damping matrix is a linear combination of Mass and Stiffness matrices, where tuning coefficients c_1 and c_2 can be opportunely defined for optimal convergence rate. Since the structural dynamics is determined by arbitrary coefficients, the evolution of the structure follows a pseudo-time step. The purpose is then to reach a steady equilibrium state for a given load, rather than to represent a real dynamics.

$$\mathbf{C} = c_1 \cdot \mathbf{M} + c_2 \cdot \mathbf{K} \quad (2)$$

The cable holding the sail (sheet) has been simulated by directly expressing the cable strain energy. The terms to be added to the right hand side and the stiffness matrix are then obtained by differentiating respectively once and twice with respect to the vector y , which stores the displacement of the constrained nodes. Using the Green-Lagrange strain measure, the the cable potential can be expressed as:

$$W_c = \frac{E_c \cdot A_c}{2} \cdot [(x_0 - x_f + y)^2 - ((1 + \epsilon)(x_0 - x_f))^2]^2 \quad (3)$$

where E_c and A_c are the Young modulus and the section area of the cable; x_0 , y and x_f are the coordinate of the cable constrained node, its displacement and the cable fixed point respectively, as specified in figure 1 *Left*. In order to avoid singularities and to respect the physics, a small circular region of the sail has been constrained rather than a single mesh point. The factor $(1 + \epsilon)$ is introduced to modify the cable's length, thus simulating a sheet ease as in figure 1 *Right*, where a 35% ease is allowed for a sail section loaded with a constant pressure load.

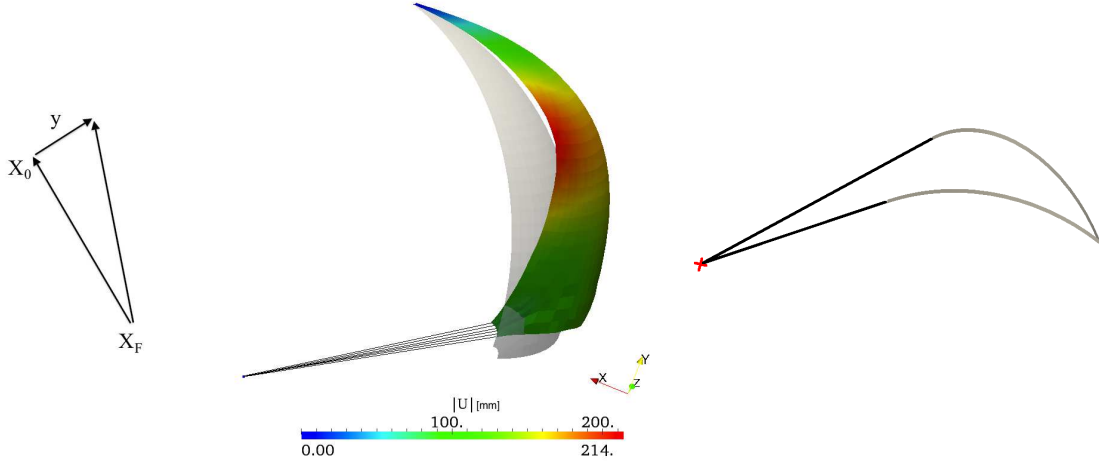


Figure 1: *Center*: A Gennaker type sail constrained with cables on one corner. In grey the sail's undeformed shape. *Right*: Deformed shape change due to a sheet ease for a two dimensional sail section with constant pressure load.

Conforming meshes are used for the coupling, therefore the structural faces are one-to-one mapped onto the fluid mesh. Δp value are exported from the fluid domain to the structural domain and integrated onto the element Gauss points. The structural displacements are interpolated from the element's nodes as: $Y^{el} = \frac{1}{4} \sum_{k=1}^4 y_i$, and the volume element displacement is assigned. Once the boundary volume element displacement is assigned, OpenFOAM offers dynamic mesh handling capabilities for the displacement of the internal mesh. It was chosen here to use the *displacementLaplacian* solver, which uses a Laplacian operator to diffuse the mesh displacement in the whole domain. The diffusivity coefficients are calculated with the *quadratic inverseDistance diffusivityCoeff (Interface)* option. The mesh motion diffusivity is tuned as a quadratic function of the distance from the moving interface, tuned by a scalar coefficient *diffusivityCoeff*. This strategy allows large mesh displacements for unchanged topology, with general conservation of the volume cell quality.

The coupling is performed via a MPI communicator. The structural solver "Program" is called from within the fluid solver using *MPI_Comm_spawn("Program", ...)*; and the point to point communication is then assured by successive call to *MPI_Send(...)*; and *MPI_Recv(...)*; within the time-step cycle.

The initialization plays an important role in the analysis. Both for the fluid and the structure in fact the steady equilibrium configuration can be far from the initial guess, and a long time can be required to reach equilibrium. This is particularly evident when large regions of separated flow and high vorticity are encountered, as in the case for downwind sails. The fluid is in fact initialized as a constant velocity field, and the analysis is carried out with the initial fixed geometry until a steady state is achieved. An example for this is reported in figure 2, where the complexity of the flow field and the long time needed for reaching a steady state are reported. In order to reduce the computational cost this phase, two main strategies can be used. OpenFOAM supporting parallel computing, the computational domain can be divided into several sub-domains. Furthermore, a coarser mesh can be used in the initialization phase, where the general flow behaviour is requested, rather than the flow details. The OpenFOAM utility *mapFields* can then be run for mapping the results on a finer mesh, to be used for the FSI.

Two major requirements should be verified for the analysis, which affect the time-step value. The mesh size is imposed by the $y^+ = u^* \frac{\Delta y}{\nu}$ value, with ν the fluid viscosity; u^* a dimensionless typical

velocity and Δy the mesh height on the wall surface. This is required to be 1 onto the sail surface in order to avoid the use of wall functions, or to be 40 and 150 for an optimal use of wall functions. This bounds the cell size onto the sail surface. Furthermore, since OpenFOAM uses uncoupled semi-implicit solvers, it is required the Courant number $Co = u_y \frac{\Delta t}{\Delta y}$ to be ≤ 1 . Δy being the smallest cell typical size, and u_y the velocity calculated in the cell, this requirements bounds the time step for a given mesh. Respecting such bounds results in very small time-steps. Taking as example the analysis in figure 2, this was run out on 24 processes decomposed domains; the time-step value for the final mesh, with $y^+ = 1$ on the sail surface was 0.002 sec. Coarser meshes in the initialization phase then allow larger time-steps and a lower computational effort for every time-step.

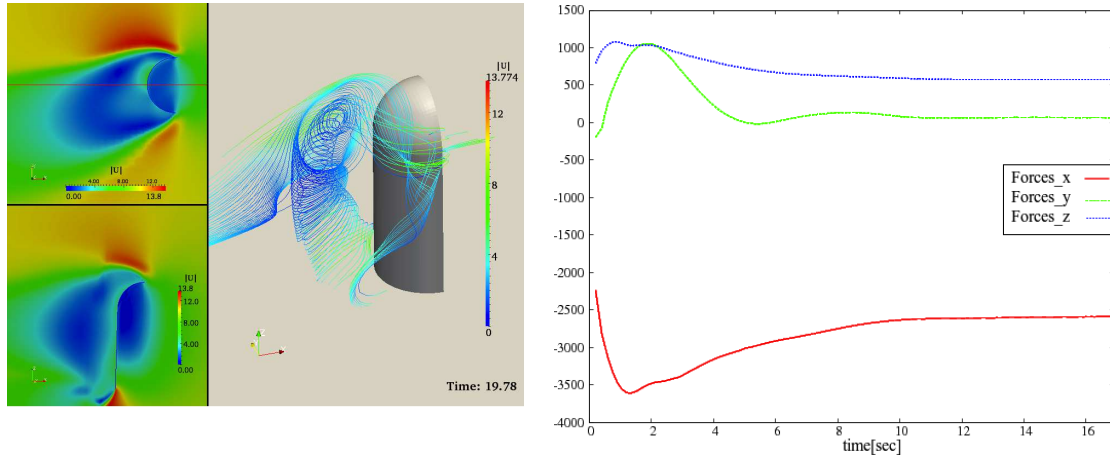


Figure 2: *Left*: The equilibrium flow field for a spinnaker type flow. *Right*: Force plot versus time.

Once a pressure field reasonably close to the equilibrium has been calculated, this can be used for the structural solver, which calculates the initial deflected position. This phase generally takes also a long time: due to the very limited thickness of the fabric and the large displacement regime, the major contribution in the device's stiffness derives from the non-linear membrane stiffness. This results in large oscillations in the firsts time steps, which are then progressively damped as the analysis proceeds. The general behavior of the structure in this phase is exemplified in figure 3, where the displacement of a sample node of the structure is reported versus the time-step.

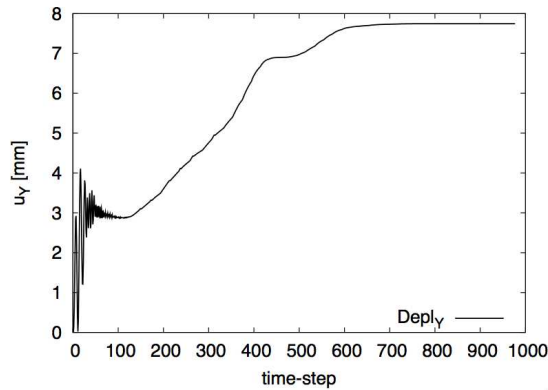


Figure 3: nodal displacement versus time-step

When the stationary equilibrium for the first load vector is reached, the displacement is assigned to the interface representing the sail in the fluid domain. This phase requires the use of under-relaxation, since large displacements can be imposed, which can introduce numerical instabilities in the calculation. The structural displacement is then linearly assigned as the fluid time proceeds. Being y_s^0 the structural displacement vector, y_F^n the displacement of the fluid interface at time-step n and α a scalar value, the relaxation is expressed as in equation 4. It was found that good values for α are of the same order of magnitude of the time-step value.

$$y_F^{n+1} = y_F^n + \alpha \cdot (y_s^0 - y_F^n) \quad (4)$$

Once the fluid mesh has reached the structural deformed shape, the FSI calculation starts in the assumption of quasi-static structural dynamics. The structural equilibrium is then verified for every fluid time step, and the formulation of equation 4 remains unchanged, but the structural displacement vector stores now the displacement updated at every time step and the relaxation factor α can be increased.

3 Results

A typical two dimensional sail section has been analysed for testing the FSI algorithm. Since the structure is represented by a developable surface, in-extensional displacements are allowed. The initial shape does therefore not play any significant role in the final deformation, which is ruled in this case by the loading and the boundary conditions only. The sail chord is 3 [m], and the sail span is 0.25 [m]: the 2D analysis is in fact realised using a one-layer-thick domain. Typical values for the analysis are reported in Table 1. The inlet velocity has been chosen in order to develop a fully turbulent flow ($Re > 10^5$), in a range typical for downwind sail analysis.

Table 1: Fluid and structural analysis constants

u [m/s]	ρ_F [Kg/m ³]	v_F [m ² /s]	ρ_S [Kg/mm ³]	v_S [-]	t_S [mm]	E_S [N/mm ²]
2.5	1.225	$1.15 e^{-5}$	$1.15 e^{-6}$	0.4	0.3	$3.76 e^{+2}$

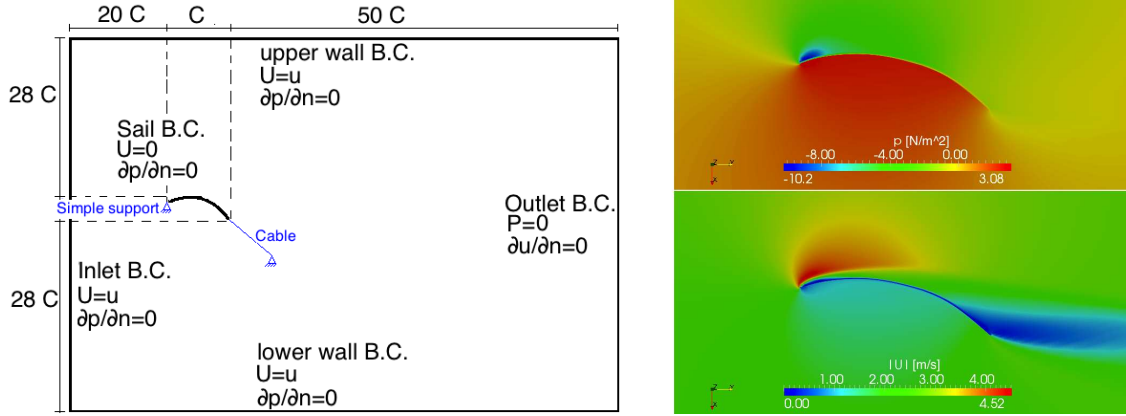


Figure 4: *Left*: Fluid domain and boundary conditions, *Right*: The fluid domain initialised for $\alpha = 13.75^\circ$

Denoting by C the wing chord length, the fluid domain extends $20 C$ in the front, $50 C$ on its back, $28 C$ over and $27 C$ under the device. Mixed Dirichlet and Neumann boundary conditions are imposed on domain outer walls and the sail surface, as summarised in figure 4. Boundary conditions for κ and ω are imposed on the sail surface using the OpenFOAM in-built wall functions, where values are assigned as: $\kappa = \frac{3}{2}(5\% \cdot U_{in})^2 = 0.0234[\frac{m^2}{sec^2}]$; $\omega = \frac{\sqrt{k}}{chord} = 0.051[Hz]$. *ZeroGradient* condition is assigned at the boundaries of the domain. The flow field is initialised on a coarse mesh composed of 3346 Hexahedra; results are mapped and continued on a finer mesh, composed of 14604 Hexahedra. y^+ values on the wing results between 11 and 470, with an average value of 150. The mesh is then suitable for using wall functions. This is acceptable in order to reduce the computational effort for the FSI, since the focus is placed on the flow general features, rather than on its details. Nine angles of attack are tested, from -6.25° to 28.75° . The device is placed with an initial angle of attack of 18.75° with respect to the domain's reference system drawn in figure 4.

The fluid initialization is run for quite a long time with a fixed geometry, in order for the flow to be really established on an equilibrium configuration. Due to the sharp edges and the curvature of the device, reaching a stable configuration is not trivial. This happens in particular in correspondence of some angles of attack (18.75°), when the flow separation is in an intermediate regime. For lower angles of attack in fact a separation bubble establishes on the leading edge, the flows then reattaches and separates again in the adverse pressure gradient region. For higher angles of attack the flow is fully separated. It should be remarked that the the length of such separation regions is in general very difficult to predict with RANS

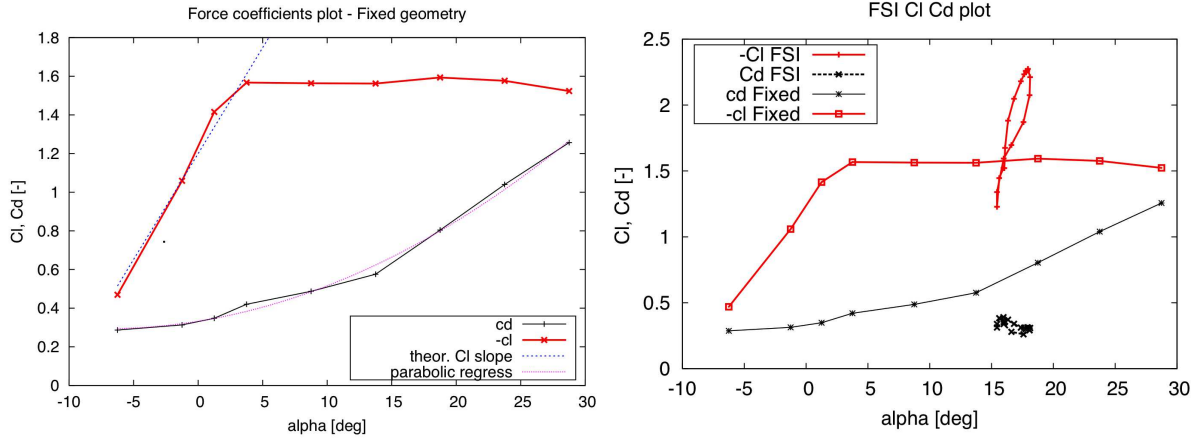


Figure 5: *Left*: Force coefficients generated on the device in the initialization phase versus the angle of attack. *Right*: Force coefficients change due to fluid structure interactions: time = 125-135 [sec].

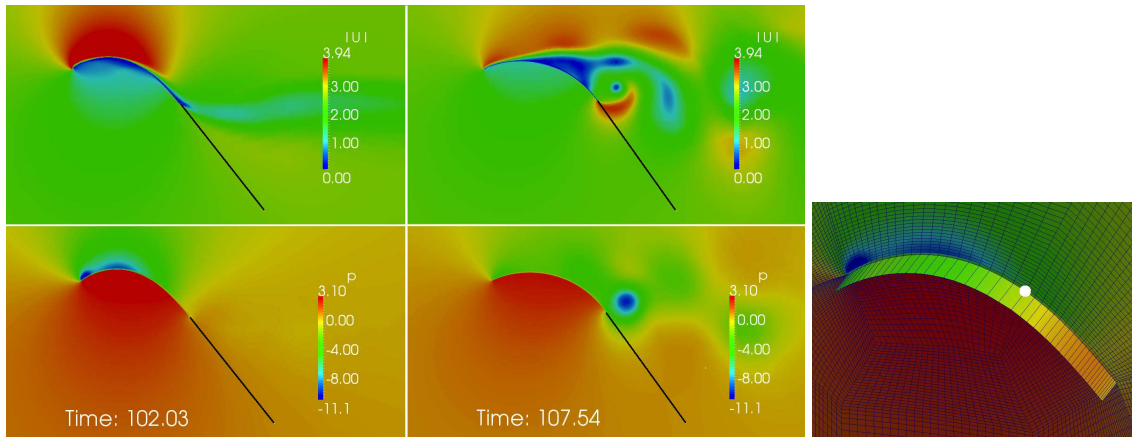


Figure 6: *Left*: Velocity and pressure field in two instants of the FSI simulation. *Right*: The point probe location (highlighted in white)

models, and that here the laminar to turbulent transition arising on the leading edge has completely been neglected. The force coefficient plot in figure 5 shows the typical behaviour of an airfoil section, where the lift coefficient $C_l = F_{\perp} / (0.5 \rho S v^2)$ has is linear with slope $\approx 2\pi$ and it remains almost constant or drops when separation arises. The drag coefficient, defined as $C_d = F_{\parallel} / (0.5 \rho S v^2)$, being F_{\perp} and F_{\parallel} the generated force projected in perpendicular and parallel direction with respect to the flow. In this case, where the airfoil is constituted by a highly cambered thin section, separation arises for very small angles of attack.

The fluid initialization field is used as starting point for the FSI analysis. The sail is held in place with a simple support on the leading edge and a cable on the trailing edge, as described in figure 4. The position of the cable's fixed point is shown in figure 6, thus the sail is free to move on a circular path with radius 5.05 [m]. Figure 5 and figure 7 report results of the analysis performed with the horizontal flow, or an angle of attack of 13.75° . The flow was completely steady in the initialisation phase with fixed geometry. Introducing the structural motions produces now unsteady vortex shedding. A periodic regime is generated ($T \approx 8sec$), where good correspondence can be found between the behaviour of the sample point displacement and the pressure value. This seems to validate the suitability of the quasi steady assumption used for structural calculations. A shift of about 0.7 sec can be identified between the pressure and the displacement signal. The periodicity of the displacement signal is confirmed by the right part of figure 7, where the (almost closed) trajectory of the sample point is drawn for the time identified by one FSI cycle (121-129 [sec]). Similar consideration can be made in terms of the force coefficients change. This is reported in figure 5, where the variation of the force coefficients is reported taking into account the change in effective the angle of attack due to the structural deformation. The lift coefficient tends to oscillate around the values obtained with the fixed geometry analysis. The drag

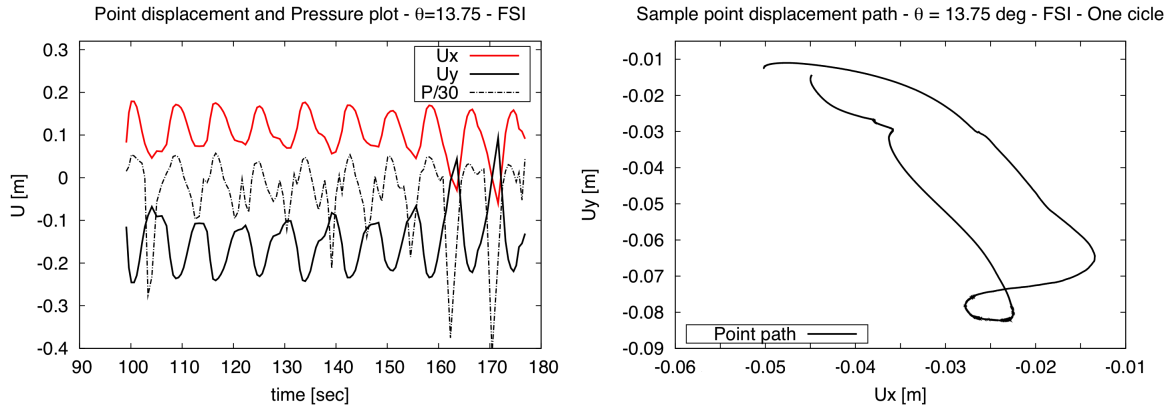


Figure 7: *Left*: Velocity and pressure field in two instants of the FSI simulation. The pressure signal has been scaled of a constant factor in order to be comparable with the displacement values. *Right*: The point probe displacements path for one FSI cycle.

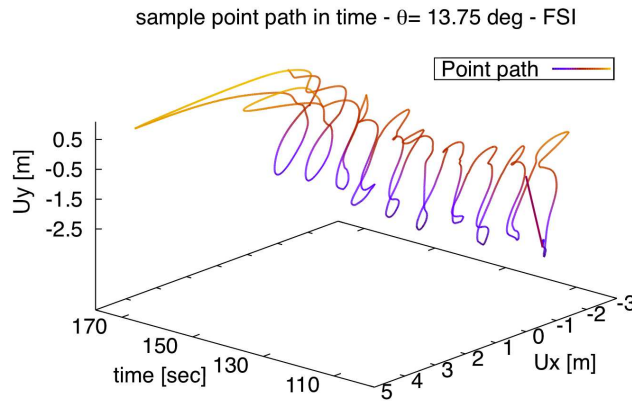


Figure 8: Point displacement path in time. The pressure peaks already identified in figure 7 *left* at the end of the calculation ($t > 160$ sec) produce large displacements of the device sample point.

coefficient results much more stable, and it drops oscillating around sensibly lower values. This is not surprising, since the fixed shape trailing edge, which faces the flow with a considerable angle, which reduces when performing FSI. The analysis has been carried out for a considerable physical time with the objective of verify the convergence capabilities of the explicit coupling algorithm in this situation. The calculation proceeds for quite a long time and it seems to be established on a periodic behaviour. However, after eight or nine periods (for $t > 160$ sec) it can be observed an increase in the pressure peaks and the structural displacements as in figures 7 *left* and 8. Continue such calculation would then result in severe convergence issues. The cause of such instability can perhaps be searched in the explicit algorithm, which does not automatically guarantee convergence. However, it should be remarked that the presented calculation is likely to be particularly unstable. From a fluid point of view, 2d unsteady calculations often force the generation of unsteady phenomena such as vortex shedding [12]. When analysing similar configuration in the three dimensional domain, the results are often much more stable, due to the mixing allowed by the extremity effects. From a structural point of view, a the analysed device is constituted by a developable surface. As stated in the beginning of this section, this means that in-extensional displacements are allowed. The presence of the cable then further extends the number of admissible solutions. The resulting system is therefore extremely ill posed, thus unstable.

4 Conclusions and future developments

The present paper shows an approach for the coupled fluid structure analysis of thin fabrics such as sails. A numerical procedure has been established, involving Finite Volumes methods with turbulence models for the analysis of the fluid domain. For the fluid analysis the OpenFOAM library has been employed.

The structural domain is analysed with shells finite elements, using the Shelddon package. The coupling is performed in an ALE framework, where the structural displacement is diffused in the fluid domain using a Laplacian operator. The structural deformation is modeled with a 'quasi static' assumption, which seems to produce acceptable results even when the flow becomes unsteady. Results have been reported and discussed for a two-dimensional sail section held in place by a simple support and a cable. The flow field has been initialised with the fixed sail section, and typical force coefficient plot have been obtained. The FSI coupled analysis has then been performed; results have been compared and discussed. In particular, the presented approach uses an explicit coupling algorithm, where the structure is analysed in the quasi-static assumption. The presented test case was representative of a critical situation, where both the fluid and the structural calculations are likely to be unstable. Despite of this, the analysis was carried out for a reasonable time with no remarkable convergence issues. It can then be concluded that the presented approach results suitable for the dynamic analysis of three dimensional sails. In the near future fully three dimensional calculations will be carried out and possibly validated with experimental data. Performing three dimensional calculation would eventually confirm the evaluation of the impact of wrinkling on the flow, which was started in [12]. From a computing perspective, several improvements can be made. In the present stage the FSI communication allows only single process calculations, thus the parallel computing capabilities of OpenFOAM are not exploited. Only conforming meshes are used, whereas different mesh distributions may be suitable for the fluid and the structural analysis.

References

- [1] K.J. Bathe. *Finite Element Procedures in Engineering Analysis*, Prentice-Hall, 1996.
- [2] D. Chapelle, K.J. Bathe. *The Finite Element Analysis of Shells: Fundamentals*, Springer, 2003.
- [3] S. Collie, M. Gerritsen, P. Jackson. *A review of turbulence modelling for use in sail flow analysis*, School of Engineering report 603, the University of Auckland, 53 pages, 2001
- [4] M. Durand, Y. Roux, A. Leroyer, M. Visonneau. *Unsteady numerical simulations of downwind sails*, Innov'Sail conference, The Royal institution of Naval Architects, 10 pages, 2010.
- [5] C. Kassiotis. *Which strategy to move the mesh in the Computational Fluid Dynamic code OpenFOAM*, Report École Normale Supérieure de Cachan. Available online: <http://perso.crans.org/kassiotis/openfoam/movingmesh.pdf>, 2008
- [6] Menter, F. R., *Two-Equation Eddy-Viscosity Turbulence Models for Engineering Applications*, AIAA Journal, Vol. 32, No. 8, pp. 1598-1605, August 1994
- [7] www.openfoam.com.
- [8] N. Parolini, A. Quarteroni. *Mathematical models and numerical simulations for the America's cup*, MOX report, Politecnico di Milano 36 pages, 2004.
- [9] H. Renschz, O. Muller, K. Graf. *FlexSail - A fluid structure interaction program for the investigation of Spinnakers* Innov'Sail conference, The Royal institution of Naval Architects, 14 pages, 2008.
- [10] H. Renschz, K. Graf. *Fluid Structure Interaction Simulation of Spinnakers - Getting closer to reality*, Innov'Sail conference, The Royal institution of Naval Architects, 9 pages, 2010.
- [11] *Shelddon* is a finite element library developed at INRIA and registered at the *Agence pour la Protection des Programmes* under ref: IDDN.FR.001.030018.000.S.P.2010.000.20600. The base of the program is open-source and available online: <http://www-rocq.inria.fr/modulef/>.
- [12] D. Trimarchi, S.R. Turnock, D. Chapelle, D. Taunton. *The use of shell elements to capture sail wrinkles, and their influence on aerodynamic load*, Innov'Sail conference, The Royal institution of Naval Architects, 12 pages, 2010.
- [13] C.G. Wang, H.F. Tan, X.W. Du, Z.M. Wan. *Wrinkling prediction of rectangular shell-membrane under transverse in-plane displacement*, International journal of Solid and Structures, Vol.44, pages 6507-6516, 2007.
- [14] Y.W. Wong, S. Pellegrino. *Wrinkled membranes: Experiments; Analytical model; Numerical simulations*, Journal of Mechanics of Materials and Structures, Vol.1, 24, 36, 34 pages, 2006.